Detailed Uncertainty Analysis for Ares I Ascent Aerodynamics Wind Tunnel Database

Michael J. Hemsch*, Jeremy L. Hanke† and Eric L. Walker‡
NASA Langley Research Center, Hampton, VA, 23681

Heather P. Houlden§
ViGYAN, Hampton, VA, 23666

A detailed uncertainty analysis for the Ares I ascent aero 6-DOF wind tunnel database is described. While the database itself is determined using only the test results for the latest configuration, the data used for the uncertainty analysis comes from four tests on two different configurations at the Boeing Polysonic Wind Tunnel in St. Louis and the Unitary Plan Wind Tunnel at NASA Langley Research Center. Four major error sources are considered: (1) systematic errors from the balance calibration curve fits and model + balance installation, (2) run-to-run repeatability, (3) boundary-layer transition fixing, and (4) tunnel-to-tunnel reproducibility.

Nomenclature

A101	Ares I configuration for the Ares I Design Analysis Cycle 2A (ADAC-2A)
A103	Ares I configuration for ADAC-2B
CAF	forebody axial force coefficient in vertical axes normalized by the nominal cross-sectional area of the first stage
C	force or moment coefficient (CNF, CAF, CPM, CRM, CSF, or CYM)
CN	normal-force coefficient in vertical axes normalized by the nominal cross-sectional area of the first stage
CM	pitching moment coefficient in vertical axes normalized by the nominal diameter and cross-sectional area of the first stage with origin at the nozzle gimbal point
C1	configuration with full protuberances
C4	configuration with no protuberances (axisymmetric)
FS	full-scale
L/D	vehicle length-to-diameter ratio
M, M_∞	free-stream Mach number
PSWT	Boeing Polysonic Wind Tunnel (St. Louis, MO)
R	range of two values (maximum – minimum)
$\bar{R}$	average range
STDEV, σ	standard deviation
UPWT	NASA Langley Research Center Unitary Plan Wind Tunnel (Hampton, VA)
Phi, φ	model roll angle
Theta, θ	model pitch angle
$\hat{\sigma}$	estimate of the population standard deviation

Introduction

This paper describes the uncertainty analysis of wind tunnel tests of two 1% scale Ares I ascent design configurations. The configurations are nearly identical in length and have identical stage diameters and aft skirts.

* Aerospace Engineer, Configuration Aerodynamics Branch, Mail Stop 499, Associate Fellow.
† Aerospace Engineer, Configuration Aerodynamics Branch, Mail Stop 499.
‡ Aerospace Engineer, Configuration Aerodynamics Branch, Mail Stop 267, Senior Member.
§ Aerospace Engineer.

Their primary differences are in the launch abort system, the blast shield covering the Orion Command Module, and the various protuberances. The identifiers for those configurations that are used in this paper are A101 for an earlier configuration and A103 for the current configuration. The designs are sufficiently different that the aerodynamics changes must be accounted for in the database. An artist's sketch of the current configuration at launch is shown in Figure 1. Note that there are three first-order loading regions for longitudinal aerodynamics: (1) crew capsule/service module, (2) interstage, and (3) aft skirt. Each protuberance creates a loading region which is second-order for longitudinal aerodynamics, but which is first-order for lateral-directional aerodynamics.

Each configuration was tested at the Boeing Polysonic blow-down wind tunnel (PSWT) for the Mach range, $0.5 \le M_\infty \le 1.6$. The PSWT testing was conducted in the transonic test section which is four-foot square and has porous walls. Each configuration was also tested at the NASA Langley Research Center Unitary Plan Wind Tunnel (UPWT) for the Mach range, $1.6 \le M_\infty \le 4.5$. The UPWT tests were conducted in two test sections: test section 1 for $1.6 \le M_\infty \le 2.0$ and test section 2 for $2.5 \le M_\infty \le 4.5$. The UPWT is continuous flow and both test sections have solid walls four-foot square. The PSWT tests used the NTF-107 force balance while the UPWT tests used the UT-39B balance. The full-scale calibration ranges (same as the maximum loading ranges) for the balances are given in Table 1. Also, given in Table 1 are the standard errors derived from the calibration curve-fit residuals. For all four tests, the force balances were attached to a straight sting which was attached to a roll motor and then to the tunnel mounting system. Base and cavity pressures were measured to correct them to free stream . Both pitch runs at constant zero roll angle and roll runs at constant pitch angles were obtained. The PSWT tests used continuous pitch and roll with data acquisition (digitization) at 100 frames a second that was post-processed with a digital filter at 20 Hz. The UPWT tests used pitch-pause and roll-pause data acquisition, acquiring data at 30 frames per second and averaging 60 frames to create a data point.

The test reports for the subsonic-to-low-supersonic tests conducted in the Boeing Polysonic Wind Tunnel (PSWT) are presented in References 1 and 2. The test reports for the moderate-to-high-supersonic tests conducted in the Langley Unitary Plan Wind Tunnel (UPWT) are presented in References 3 and 4. Earlier work for just the repeatability portion of the uncertainty quantification for the A101 tests, using a somewhat different strategy, is presented in References 5 and 6. In the present work, the 6-DOF force and moment coefficients are analyzed in the vertical axis system which is defined such that the normal force is in the plane formed by the wind and the model axis and is opposite in sign to gravity. Figure 2 shows the orientation of the force and moment coefficients in a cross-flow plane perpendicular to the model axis and looking forward (upwind).

Database Construction

It has been found throughout Ares I wind tunnel testing that the balances required to meet the longitudinal loading requirements are too insensitive (as a fraction of full-scale load capability) for the rolling-moment measurement requirements. This is not too surprising given the high fineness ratio of a finless launch vehicle. Furthermore, it was found that mounting misalignments between the model and the balance and the balance and the sting were sufficiently large to induce unacceptable systematic roll-moment errors. However, it has also been found that the repeatability of the lateral-directional measurements for both tunnels is much better than the curve-fit errors of Table 1. Hence, a strategy was developed to take advantage of the good repeatability and allowing for subtraction of the systematic errors.

The configurations of interest for the ascent aero databases (C1, full protuberances) are not axisymmetric due to the addition of various protuberances. To account for most of the potential systematic errors in the tests, the databases are constructed to use the results from a nominally axisymmetric model (C4) and to invoke symmetry or anti-symmetry as appropriate. It is assumed that there is no error in this assumption. The buildup equation is as follows where C is one of the six force or moment coefficients:

$$C(\theta, \varphi) = C(\theta, \varphi = 0) + \Delta C(\theta, \varphi) \tag{1}$$

The first term on the right-hand side of eq.(1) is generated using pitch runs at $\varphi = 0$ which also counts, of course, for $\varphi = 360^\circ$. For the C response surface, these runs also apply for $\varphi = 180^\circ$ with a proper transformation since the data are obtained at negative as well as positive pitch angles. The second term is obtained with roll runs at four discrete pitch angles. For the A101 configuration tests, those angles were $\theta = 0, 2^\circ, 4^\circ, 7^\circ$. For the A103

configuration tests, the angles were $\theta = 0, 4^\circ, 7^\circ, 8^\circ$. For the work reported herein, the uncertainties were estimated for the pitch runs and for the roll runs at $\theta = 7^\circ$ at which almost all the roll run replicates were obtained.

The pitch run term in eq. (1) is constructed as follows:

$$C(\theta, \varphi = 0) = C1(\theta, \varphi = 0) - C4(\theta, \varphi = 0) + C4_{adjusted}(\theta, \varphi = 0) \tag{2}$$

The third term in eq.(2) is obtained from the $C4$ pitch runs adjusted for symmetry, anti-symmetry, and axisymmetry as appropriate. This is carried out for the database generated by translating the normal-force and pitching-moment results so that they go through zero at $\theta = 0$ and are anti-symmetric about zero. The axial force results are adjusted to be symmetric about $\theta = 0$. The rolling moment for the third term in eq.(2) is set to zero.**

The roll run term in eq.(1) is constructed as follows:

$$\Delta C(\theta, \varphi) = C1(\theta, \varphi) - C4(\theta, \varphi) - \left[C1(\theta, \varphi = 0) - C4(\theta, \varphi = 0)\right]_{roll\ runs} \tag{3}$$

For this term, adjusted results for the $C4$ axisymmetric configuration would be expected to be zero, i.e. no roll effects are to be expected.

The uncertainties to be considered in this analysis are evaluated in the following four steps:

1. **Interpolation residuals.** In order to carry out the arithmetic in Eqs.(1-3), it is necessary to interpolate in the experimental runs to the nominal pitch and roll angles. The residuals at the actual pitch and roll angles are analyzed to estimate potential uncertainties associated with the interpolation. All of the runs made for the database were plotted and visually inspected for errors and anomalies. For all of the runs, the interpolation errors were insignificant compared to the repeatability scatter and no anomalies were found.
2. **Within-test repeatability.** During the wind tunnel tests, replicates were obtained at selected Mach numbers for the pitch runs and for roll runs primarily at $\theta = 7^\circ$. These replicates are used to estimate the within-test repeatability. The results were also checked for anomalies using upper limits based on an assumed number of degrees of freedom and 99% confidence level based on the assumption of sampling from a Normal distribution.††
3. **Boundary-layer tripping strategy (grit) effects.** Work carried out in a test[7] for an earlier configuration was not able to determine if the baseline boundary-layer tripping strategy used in the two tunnels was adequate to cause appropriate boundary-layer transition and create the desired fully-turbulent flow state around the model. In addition, it was found in that work that different tripping strategies could have a significant effect on the force and moment coefficients. Hence, for the A101 and A103 tests in the two tunnels, pitch and roll runs were made at selected Mach numbers using a very heavy application of transition material and no transition material at all in addition to the canonical runs with baseline transition. The variation from these results together with the baseline results were used to estimate uncertainties associated with the boundary-layer tripping strategy.
4. **PSWT-to-UPWT variation for M = 1.6.** No tunnel has perfectly uniform and interference-free flow. Hence, it can be expected that testing in different tunnels might produce significantly different results compared to each tunnel's repeatability. The test matrices for the PSWT and the UPWT were designed to overlap at $M_\infty = 1.6$ to investigate this effect. However, it was not possible to test at the same Reynolds numbers in the two tunnels (the PSWT value was about 1.75 times that of the UPWT). Furthermore, the PSWT tests used trip dots to initiate boundary-layer transition for the baseline runs while the UPWT tests used grit strips. Hence, the potential variation across the two sets of tests may include all of those effects.

Steps 1-4 were applied for all four tests. Note that balance errors are not included. The within-test repeatability includes the balance repeatability and any residual systematic errors from the balance calibration are assumed to be cancelled with the approach of Eqs.(1-3). This assumption may be strained, however, for the rolling-moment coefficients since the balance is lightly loaded for this measurement.

** Because the configuration is very slender (L/D > 25) and because of the presence of the frustum and protuberances, it is possible that asymmetric flow could develop even for the relatively small pitch angles expected during ascent. Unfortunately, such flows are notoriously difficult to predict because of their extreme sensitivity to small changes in geometry, tunnel conditions, and so on. The side-force and yawing-moment uncertainties will not be analyzed for this paper. The results can be found in the references.

†† This is not a strong requirement.

Within-Test Repeatability

After interpolation in each run to the selected nominal angles, the repeatability associated with each pair of replicate runs was estimated using a robust measure. For each pitch or roll angle as appropriate, the absolute value of the difference between the replicate values (range, R) was computed. Then the average range was computed for a given replicate run set and the standard deviation was estimated as follows: [8]

$$\hat{\sigma} = 0.8865\,\bar{R} \tag{4}$$

The results for all of the replicate run sets for both the A101 and A103 configurations are given in Figures 3-6. The results for the two tunnels used are shown separately in the (a) and (b) portions of the Figures. Also shown in the plots of Figures 3-6 are the $\hat{\sigma}$ averages. These values give the best pooled estimates for the repeatability at each Mach number. Earlier work[5, 6] showed that the repeatability in the two tunnels is not a function of pitch or roll angle. Also shown in the plots is an upper limit based on assuming roughly 10 degrees of freedom[‡‡] for each replicate run pair ($limit = 2.15\,\hat{\sigma}_{average}$). For the value of the limit used and sampling from a classic Normal distribution, only 1 out of 100 standard deviations would be expected to be outside the limits. Although a few of the repeatability standard deviations are somewhat above the limits, this can be expected by chance[§§] and the averages can be safely used as estimates of the repeatability at any given Mach number for all of the replicate run sets

Note that, for the combined database uncertainties, the repeatability variances are counted four times to account for the four runs of C1 and C4 in Eqs.(2, 3). The adjusted values and zeros are not counted for repeatability.

Grit Effects

Grit effects were estimated by comparing the repeatability of the combined grit and repeatability run sets for a given condition and comparing that result with the result from the repeat run set alone. The grit effect standard deviation was considered to be the square root of the difference in variances between the combined grit and repeatability runs and the repeatability runs alone:

$$\hat{\sigma}_{grit\,effect} = \sqrt{\sigma^2_{grit+repeatability} - \sigma^2_{repeatability\,alone}} \tag{5}$$

The results are given in Figures 7-10. Note that gritting effect runs were only made for $M_\infty = 0.9, 1.2, 1.6, 2.0, 2.5, 4.0$. For $M_\infty = 0.5, 0.8$, there are no data and it is assumed that the grit effect for those Mach numbers is zero. For all other non-canonical Mach numbers, interpolation or extrapolation was used. The upper limit used as a check is the same used for the repeatability since it was measured the same way. However, for conservatism, if the maximum value at a Mach number was above the limit, the limit was set equal to that value and the average re-calculated to be $\hat{\sigma}_{average} = \sigma_{limit} / 2.15$.

For the combined database uncertainties, the grit effect variances were counted once for Eq.(2) and once for Eq.(3) for a total of twice.

PSWT-to-UPWT Variation for M = 1.6

A null hypothesis test[8] for the two means, PSWT and UPWT, can be constructed as follows. Define

$$Z_0 = \frac{C_{PSWT} - C_{UPWT}}{\sqrt{\sigma^2_{PSWT} + \sigma^2_{UPWT}}} \tag{6}$$

We will reject the hypothesis that the two means are statistically equal (null) if

$$|Z_0| > Z_{\alpha/2} = 3 \tag{7}$$

Eqs.(6, 7) are equivalent to setting a three-sigma upper limit for the absolute value of the difference between the two means to be

$$|C_{PSWT} - C_{UPWT}| = 3\sqrt{\sigma^2_{PSWT} + \sigma^2_{UPWT}} \tag{8}$$

[‡‡] Although each pitch and roll run consisted of roughly 20-25 data points, it would be expected that some autocorrelation would occur and 10 degrees of freedom seems a reasonable compromise to estimating upper bounds for the purpose of finding gross outliers.

[§§] While a classic Normal distribution typically represents wind tunnel repeatability well, in the author's experience the actual distributions typically also have somewhat heavy tails which would cause even more points to be outside the theoretical limits without negating the general validity of the analysis.

The σ values used in Eq.(8) were obtained using the repeatability standard deviations for the averages of two runs since there were two replicates for all $M_\infty = 1.6$ pitch runs and roll runs at $\theta = 7^\circ$.

For convenience in interpreting the results, the signed differences are plotted with the bounds shown positive and negative.[***] The results for both the A101 and A103 test sets are shown in Figures 11-14. The pitch runs are all for a roll angle of zero degrees while the roll runs are all for a pitch angle of seven degrees. The following observations are drawn:

1. For the longitudinal coefficients (CNF, CAF, CPM), there is only one point (barely) outside the 3-sigma limits. Hence, the null hypothesis should not be rejected. That is, there is insufficient evidence to state that there are significant differences between the two tunnel test results.
2. For the rolling-coefficient, there are only a few points lying somewhat outside the 3-sigma limits. Since wind-tunnel measurement normal distributions that are derived using robust estimators for the standard deviations match the core of the distributions well but often predict tails that are not extensive enough, it does not seem necessary to reject the null hypothesis.

Concluding Remarks

As described above, a detailed uncertainty analysis for the Ares I ascent aero wind tunnel database has been developed. The analysis has also been used for wind-tunnel databases derived for two earlier configurations. The methods used are standard statistical techniques. However, the techniques are not yet common in aerodynamic testing and analysis. The key techniques used herein are:

1. A robust measure of the repeatability based on the range. This method is typically used in statistical process control.[8, 9]
2. Quantitative verification of the homogeneity of the scatter sets using limits. This method is also used in statistical process control.[9]
3. Quantitative hypothesis testing for tunnel-to-tunnel variation.[8]

The methods described in the paper are also being used for other wind-tunnel derived databases in Ares I, Ares I-X and Orion projects.

Acknowledgements

The authors gratefully thank the PSWT and UPWT staffs and the NASA experimentalists, G. E. Erickson, F. J. Wilcox and W. G. Tomek for their outstanding work in planning and executing the wind tunnel tests analyzed in this report.

References

1. Tomek, William G., "Wing-Tunnel Investigation of a 1% Scale Crew Launch Vehicle (DAC-2A) Configuration in the Boeing Polysonic Wind Tunnel – Integrated Force and Moment Test," NASA Ares-AD-TA-0003, Released July 31, 2007.
2. Hanke, Jeremy L., "Test Summary for 1%-Scale CLV ADAC-2B (A103) Force and Moment Model Testing in the Boeing Polysonic Wind Tunnel," NASA Ares-TA-0010, Released January 8, 2008.
3. Erickson, Gary E., "0.01-Scale CLV DAC-2A Force and Moment Model Testing in the NASA Langley Research Center Unitary Plan Wind Tunnel," NASA Ares-AD-TA-0004 Released July 2, 2007.
4. Erickson, Gary E., "0.01-Scale CLV DAC-2B (A103) Force and Moment Model Testing in the NASA Langley Research Center Unitary Plan Wind Tunnel," NASA Ares-AD-TA-0009 Released December 14, 2007.
5. Houlden, Heather P.,"Characterization of Within-Test Repeatability for Boeing PSWT 839 (Ares I ADAC-2A)," NASA Ares-AD-TA-007, Released September 18, 2007.
6. Hemsch, Michael J., "Characterization of Within-Test Repeatability for LaRC UPWT Tests 1813 and 1968 (Ares I ADAC2A)," NASA Ares-AD-TA-0006, Released August 20, 2007.
7. Erickson, Gary E., "0.01-Scale CLV DAC-1 Pressure Model Testing at Supersonic Speeds in the NASA Langley Research Center Unitary Plan Wind Tunnel," April 2007.
8. Montgomery, Douglas C., *Introduction to Statistical Quality Control*, 3rd Ed., Wiley 1996.
9. Wheeler, Donald J., *Making Sense of Data: SPC for the Service Sector*, SPC Press, 2003.

[***] Note that this criterion is equivalent to putting limits on the differences.

Table 1. Force balance maximum loads and calibration curve-fit errors.				
	NTF-107 (PSWT)		UT-39B (UPWT)	
Coefficient	Full-Scale Calibration Range	Calibration Curve-Fit Standard Error, % FS	Full-Scale Calibration Range	Calibration Curve-Fit Standard Error, % FS
Normal Force, lbf	160	0.03	150	0.02
Axial Force, lbf	50	0.03	40	0.02
Pitching Moment, in-lbf	250	0.03	200	0.015
Rolling-Moment, in-lbf	100	0.1	30	0.23
Side Force, lbf	125	0.03	100	0.03
Yawing Moment, in-lbf	80	0.04	75	0.02

Figure 1. Artist's sketch of an Ares I configuration just after launch.

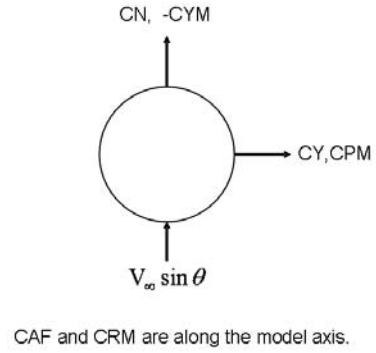

Figure 2. Vertical axis system used in the report. The view is looking forward (upstream).

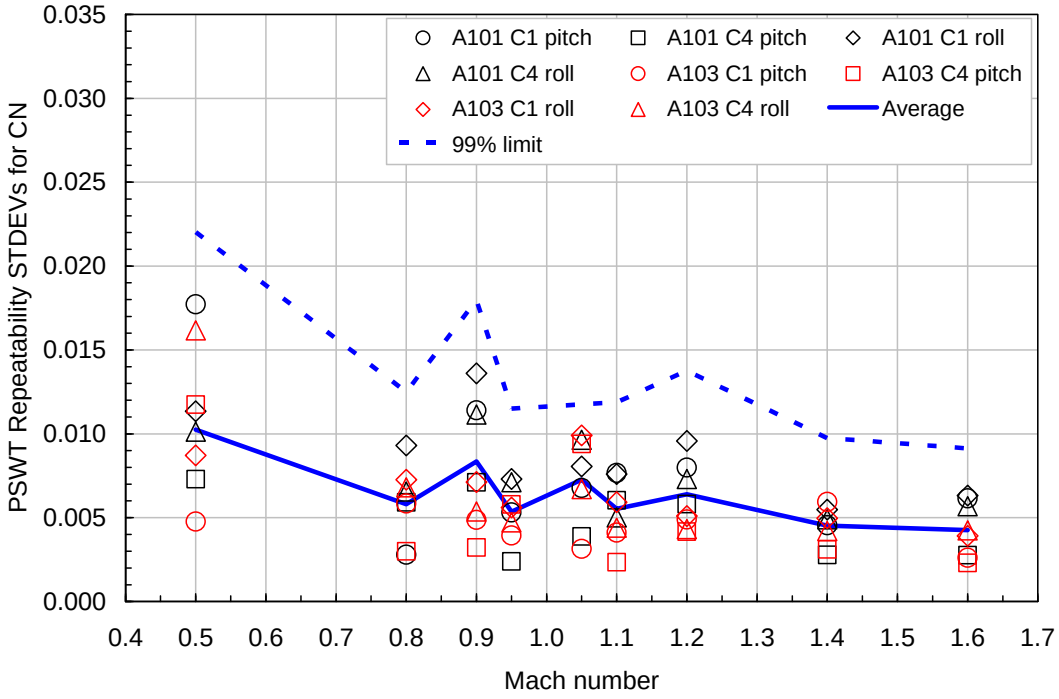

(a) PSWT

Figure 3. Mach number dependence of the repeatability standard deviations for CN together with the average interpolation standard deviations.

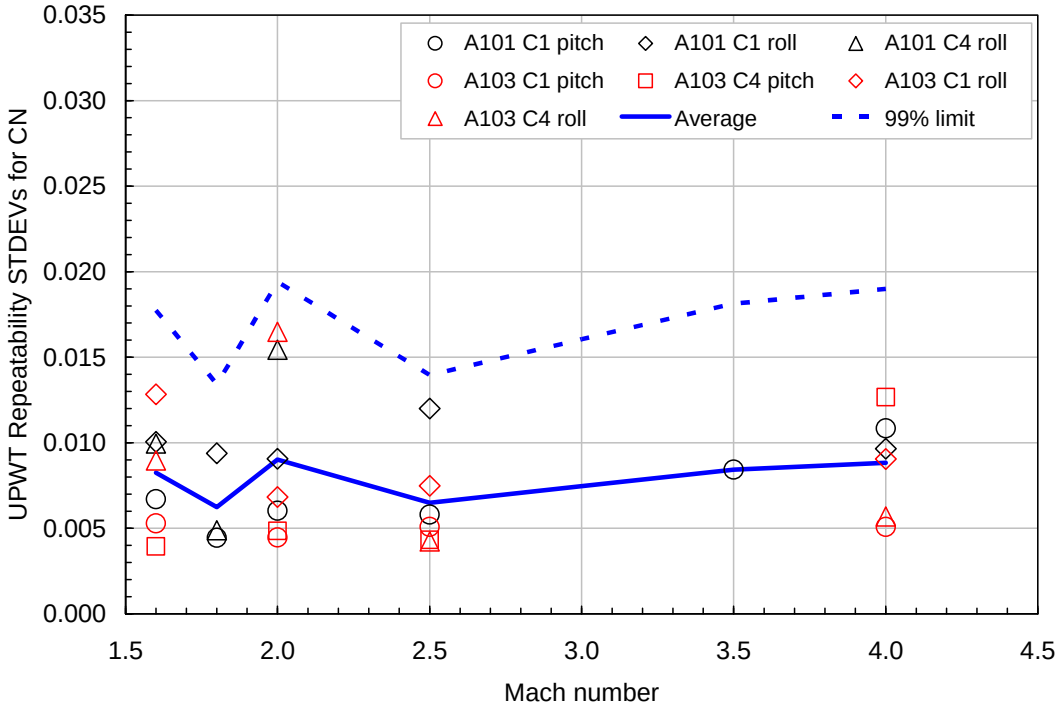

(b) UPWT

Figure 3. Concluded

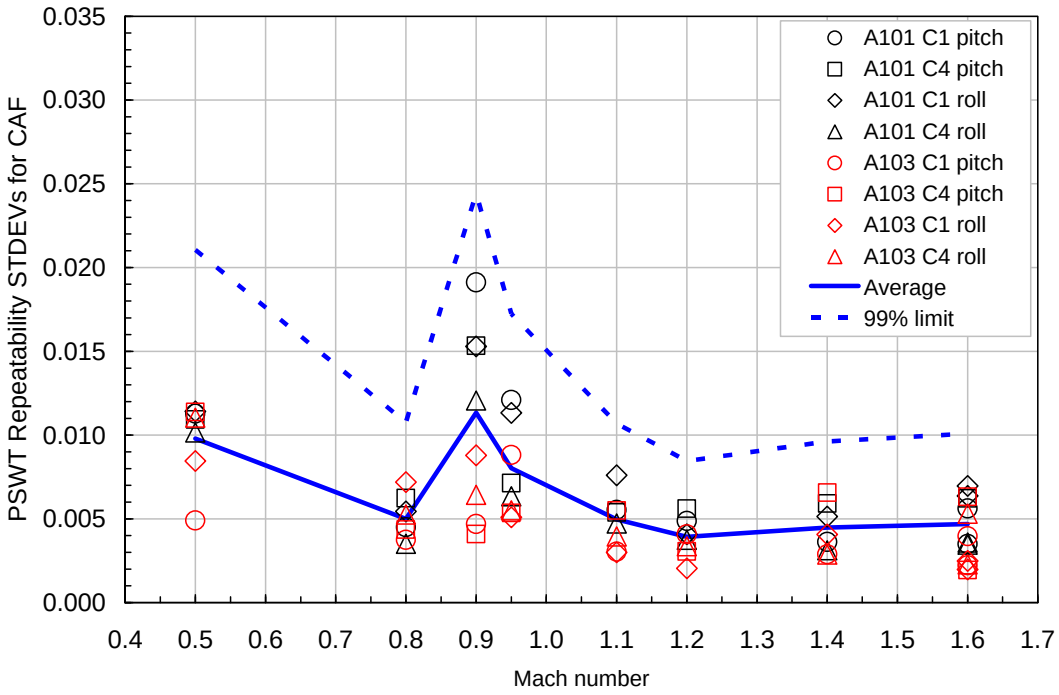

(a) PSWT

Figure 4. Mach number dependence of the repeatability standard deviations for CAF .

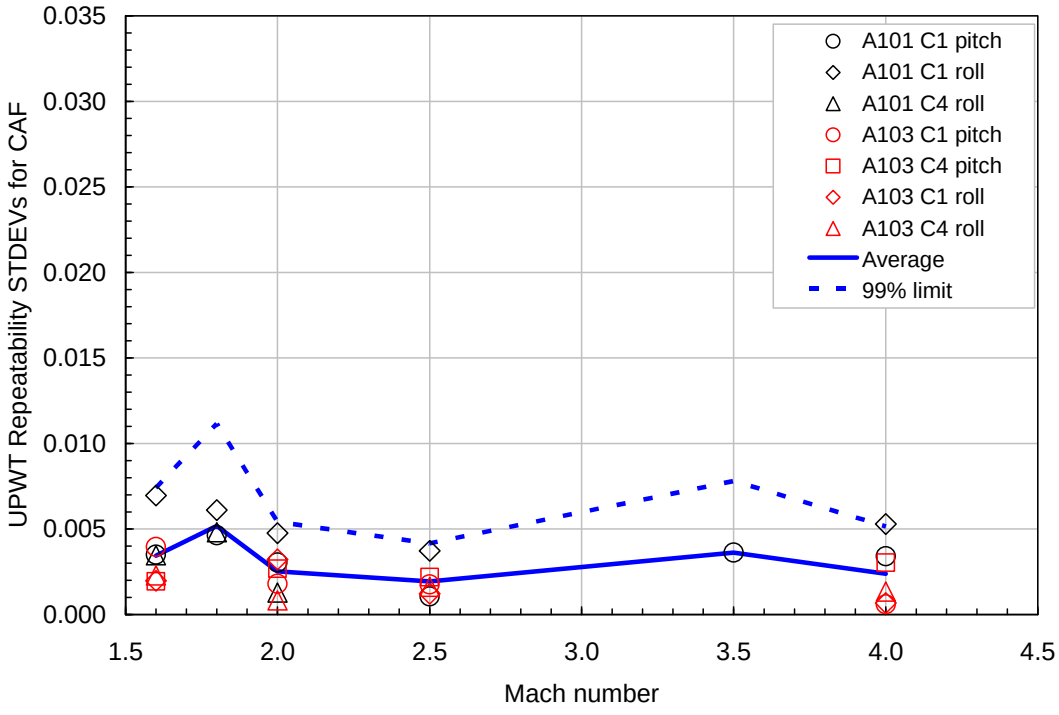

(b) UPWT

Figure 4. Concluded

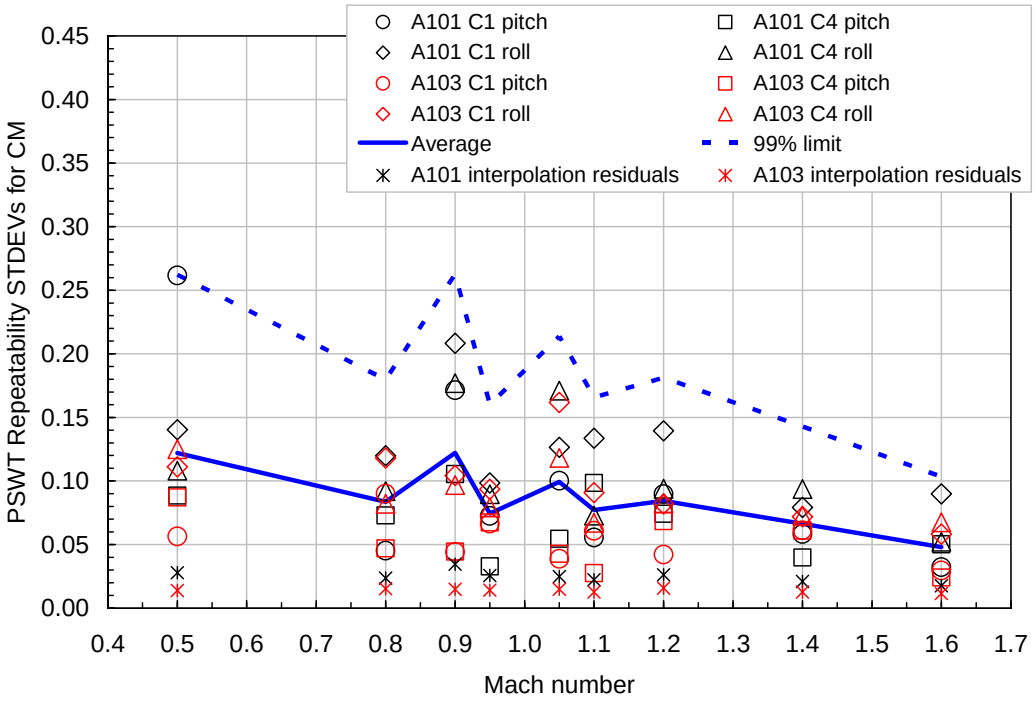

(a) PSWT

Figure 5. Mach number dependence of the repeatability standard deviations for CM together with the average interpolation standard deviations.

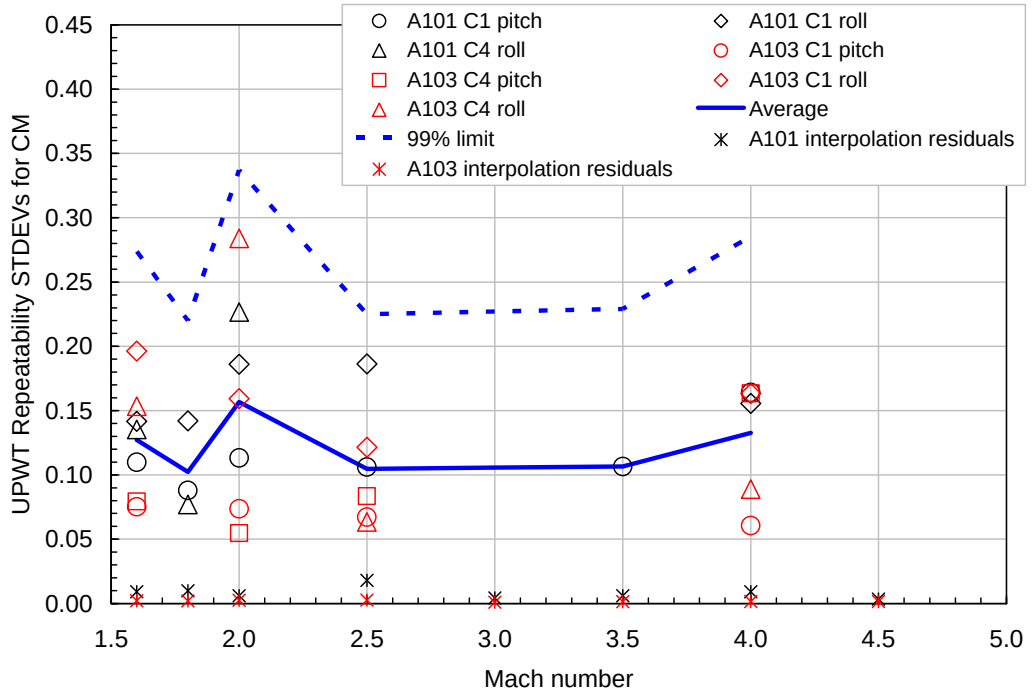

(b) UPWT

Figure 5. Concluded

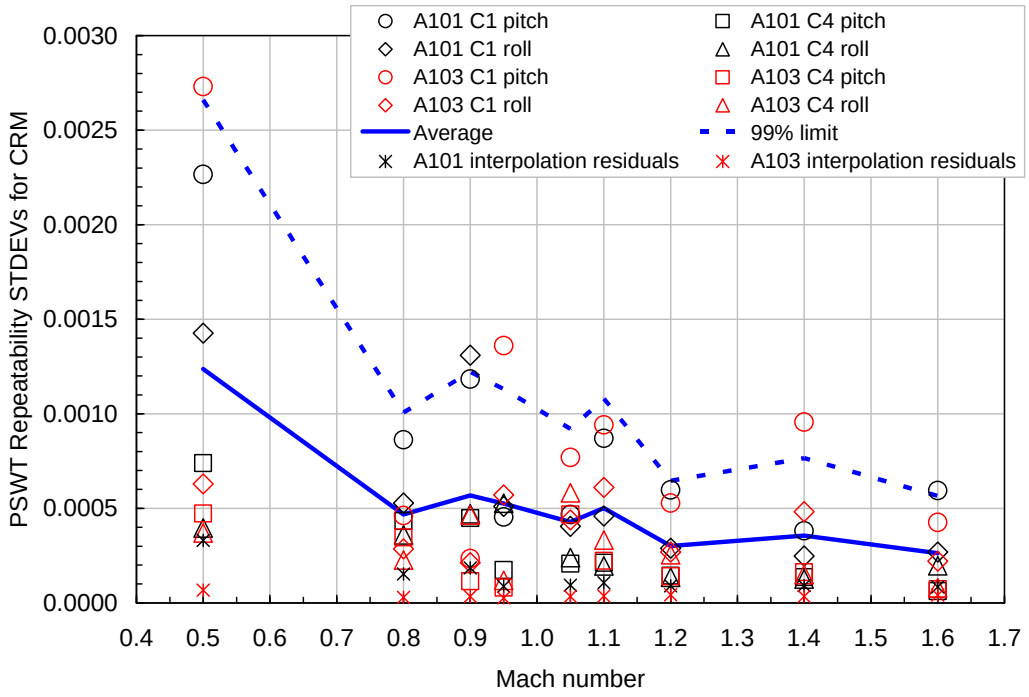

(a) PSWT

Figure 6. Mach number dependence of the repeatability standard deviations for CRM together with the average interpolation standard deviations.

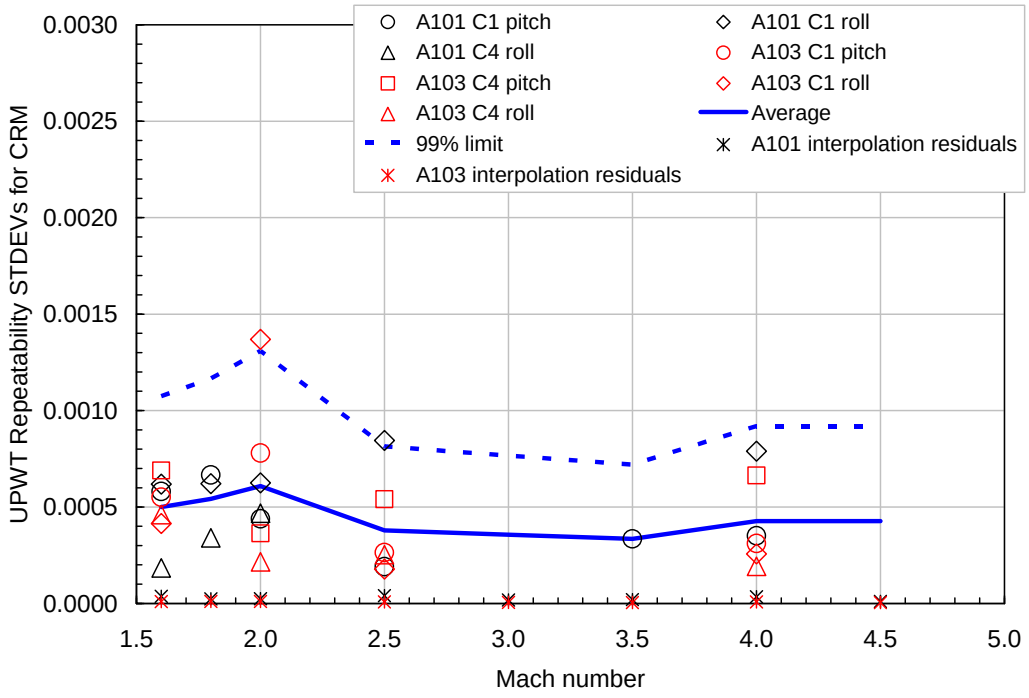

(b) UPWT

Figure 6. Concluded

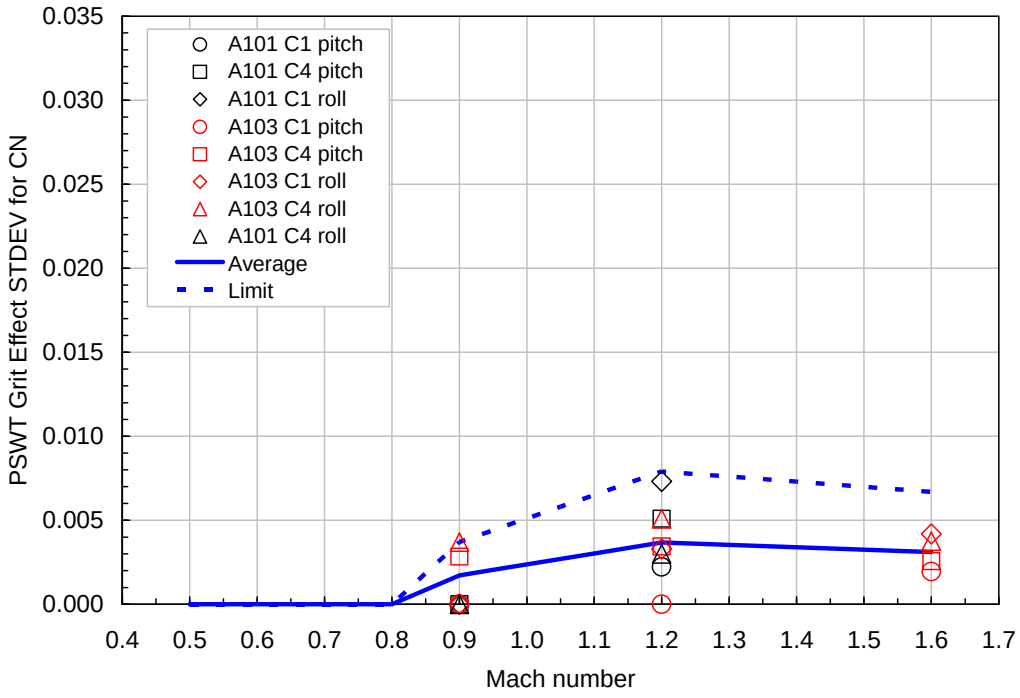

(a) PSWT

Figure 7. Mach number dependence of the gritting effect standard deviations for CN.

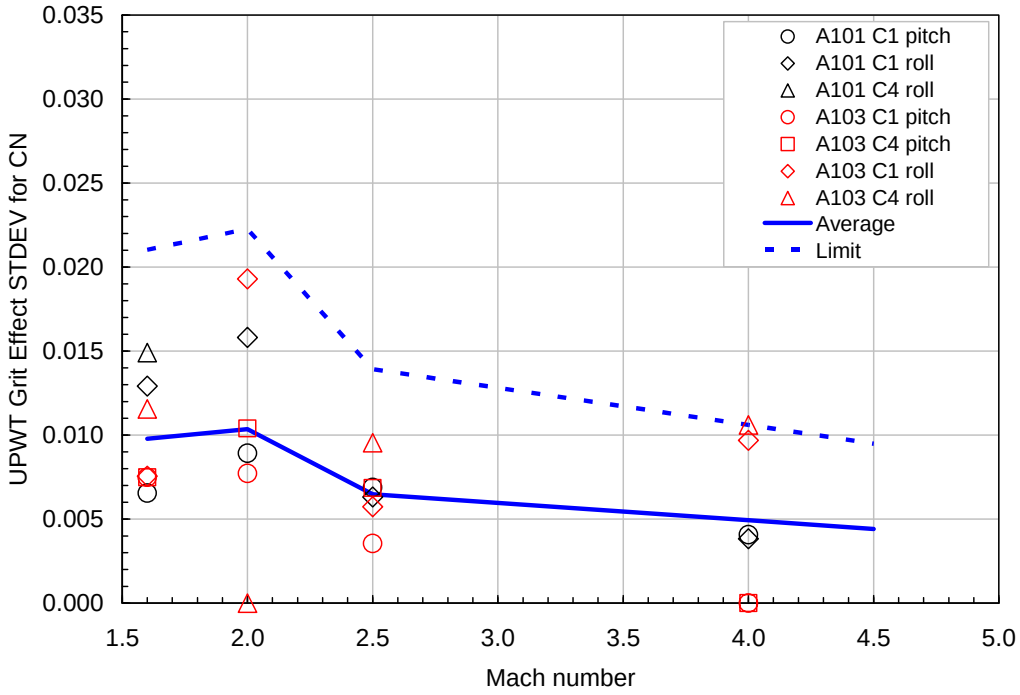

(b) UPWT

Figure 7. Concluded

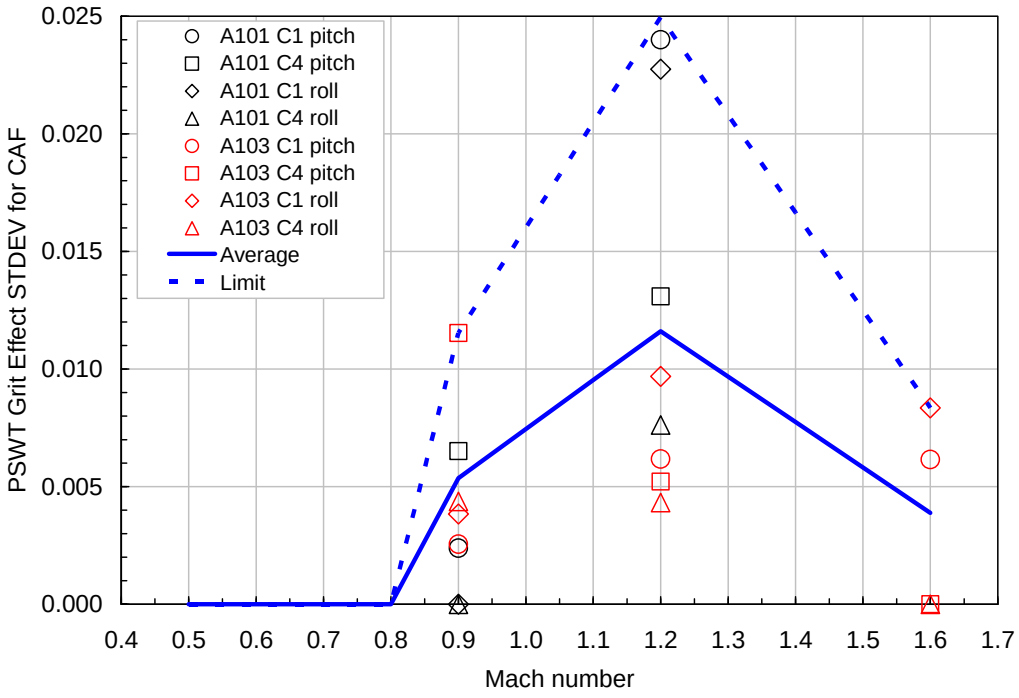

(a) PSWT

Figure 8. Mach number dependence of the gritting effect standard deviations for CAF.

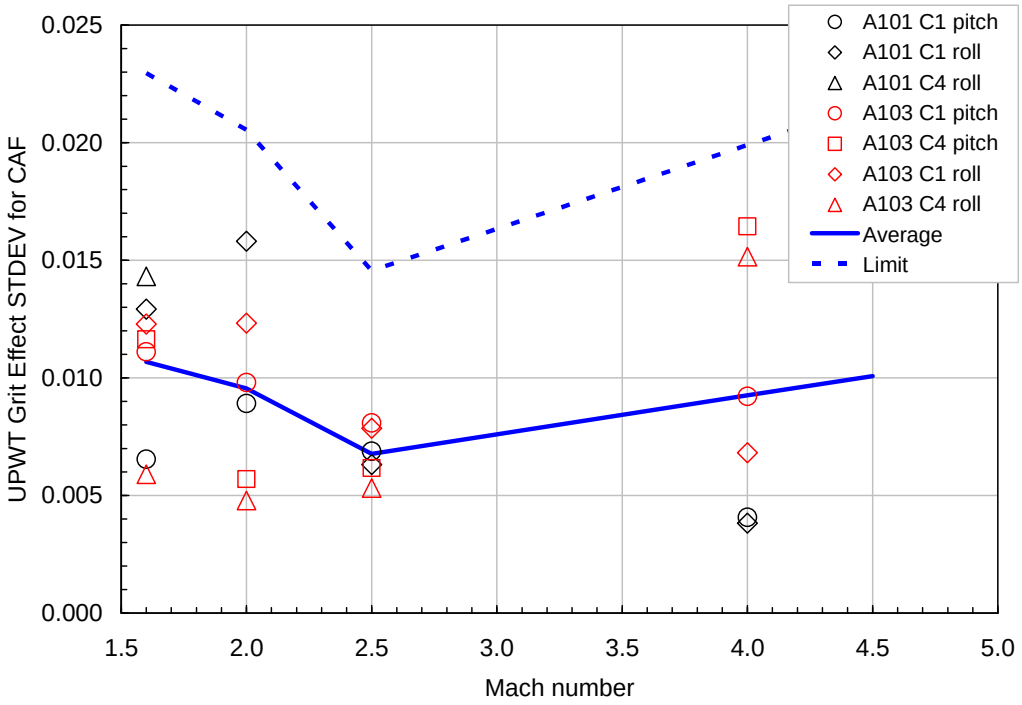

(b) UPWT

Figure 8. Concluded

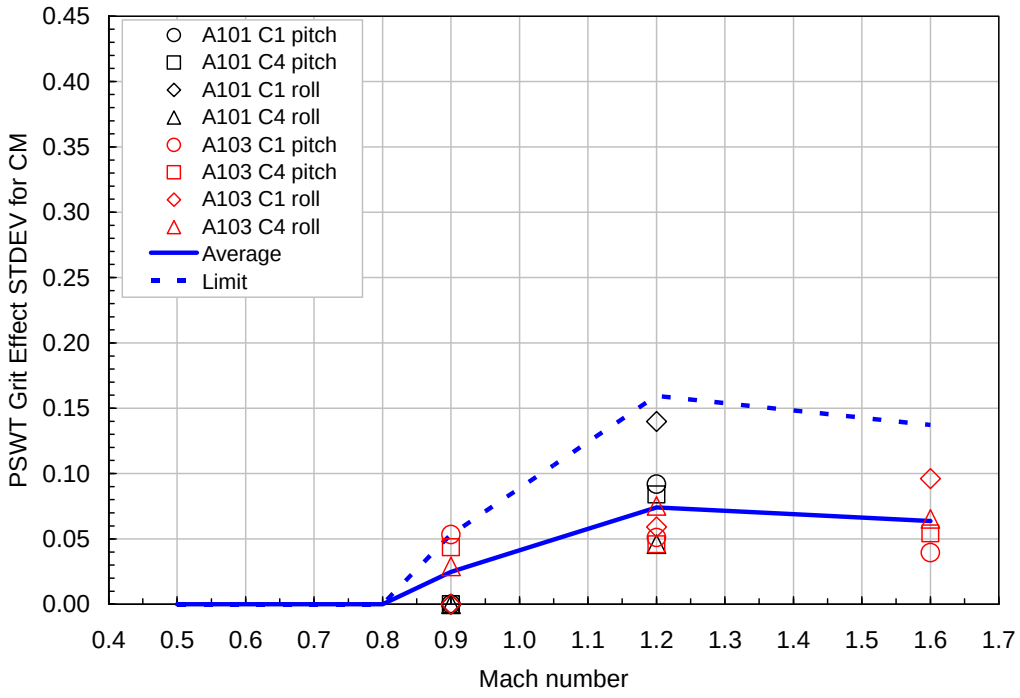

(a) PSWT

Figure 9. Mach number dependence of the gritting effect standard deviations for CM.

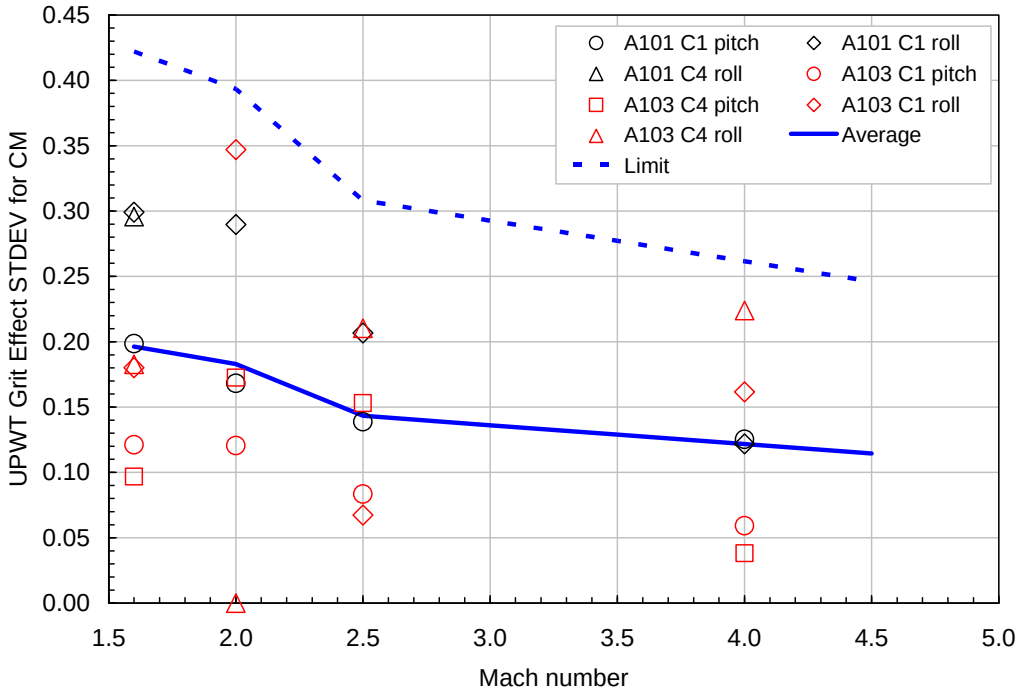

(b) UPWT

Figure 9. Concluded

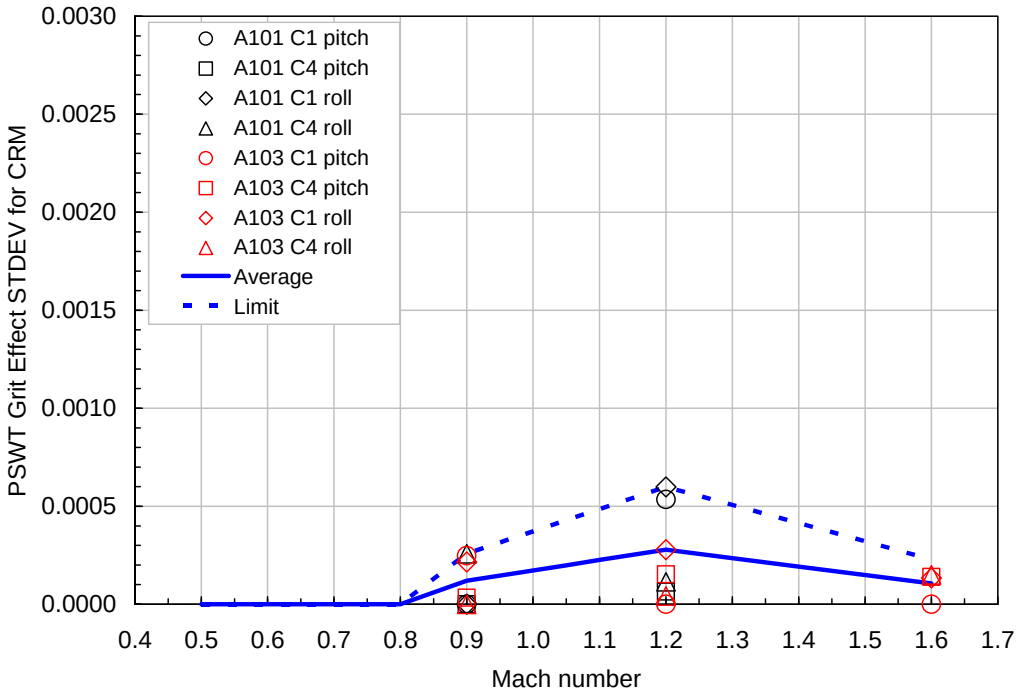

(a) PSWT

Figure 10. Mach number dependence of the gritting effect standard deviations for CRM.

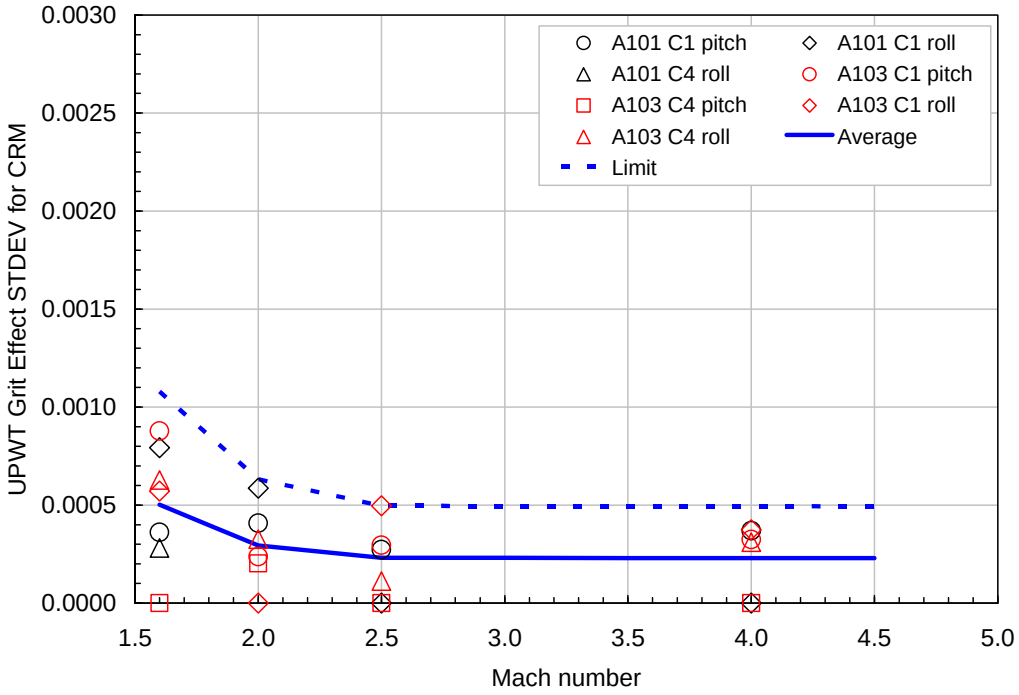

(b) UPWT

Figure 10. Concluded

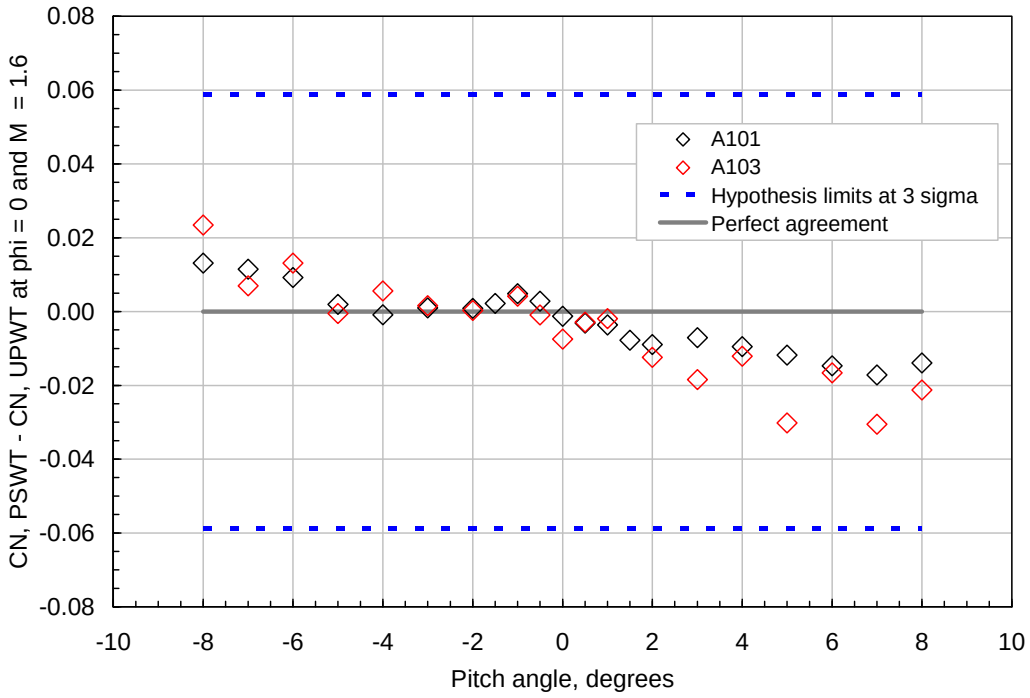

(a) Pitch runs at $\varphi = 0$.

Figure 11. CN PSWT-to-UPWT Comparison with Hypothesis Test.

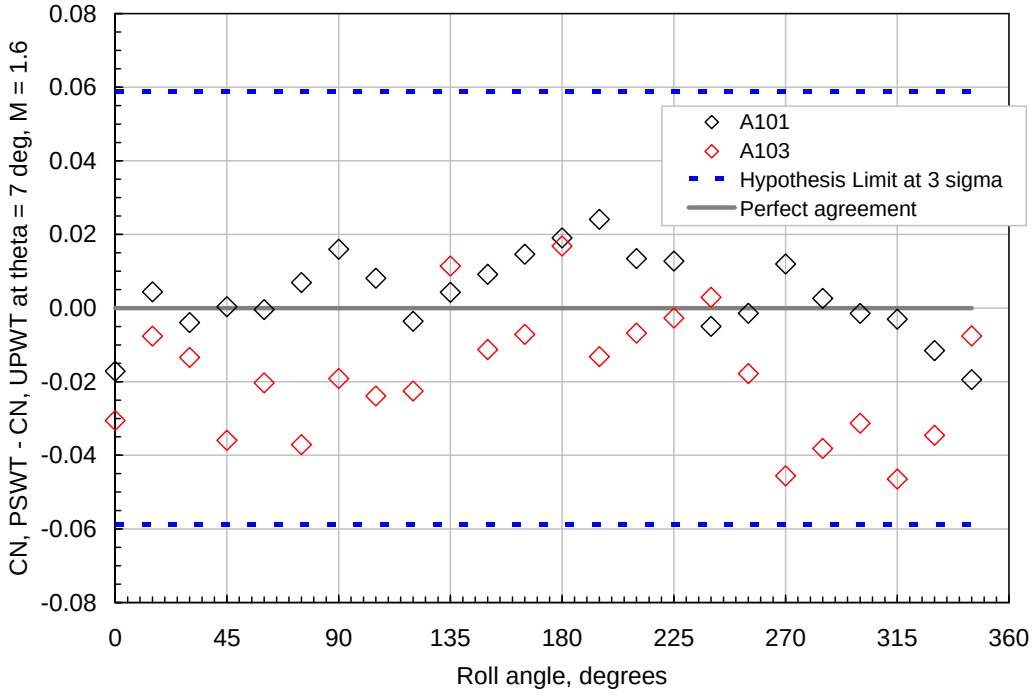

(b) Roll runs at $\theta = 7^{\circ}$.

Figure 11. Concluded.

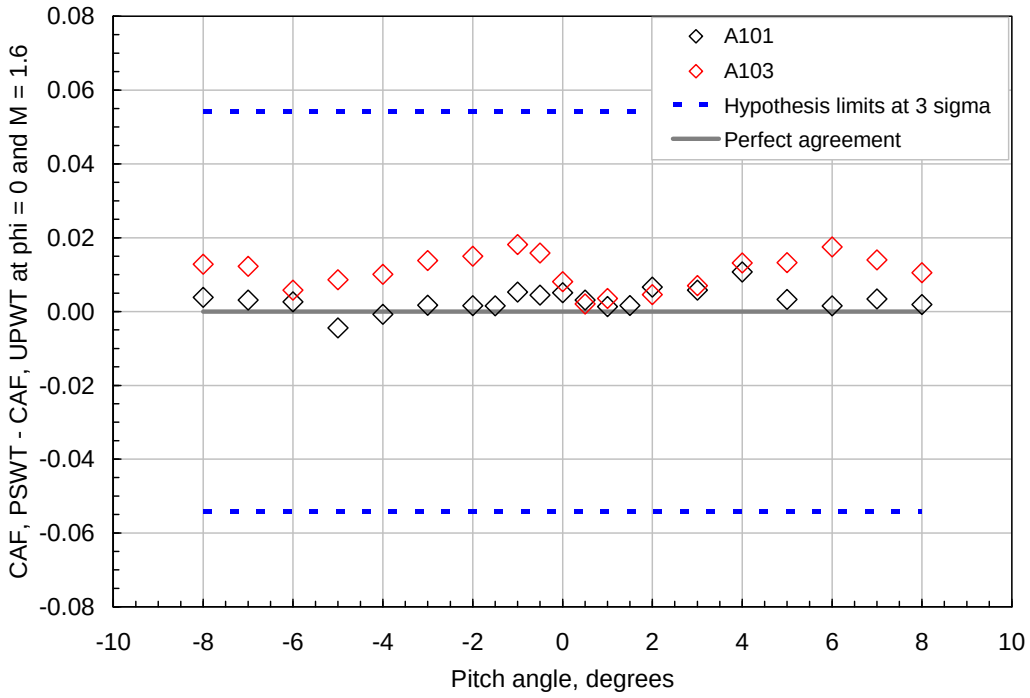

(a) Pitch runs at $\varphi = 0$.

Figure 12. CAF PSWT-to-UPWT Comparison with Hypothesis Test.

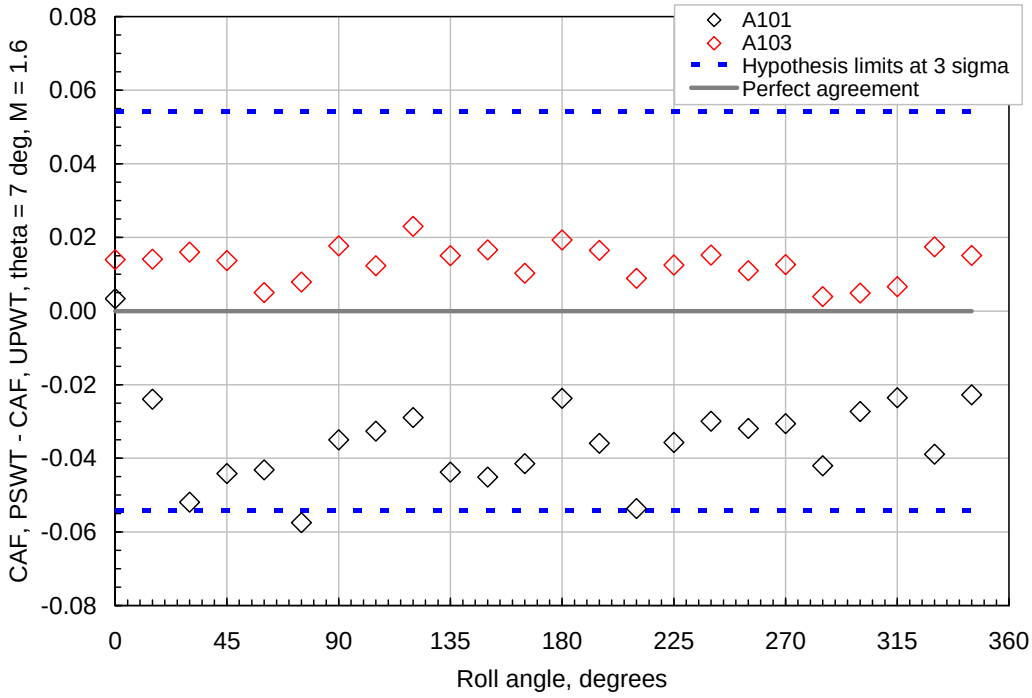

(b) Roll runs at $\theta = 7^{\circ}$.

Figure 12. Concluded.

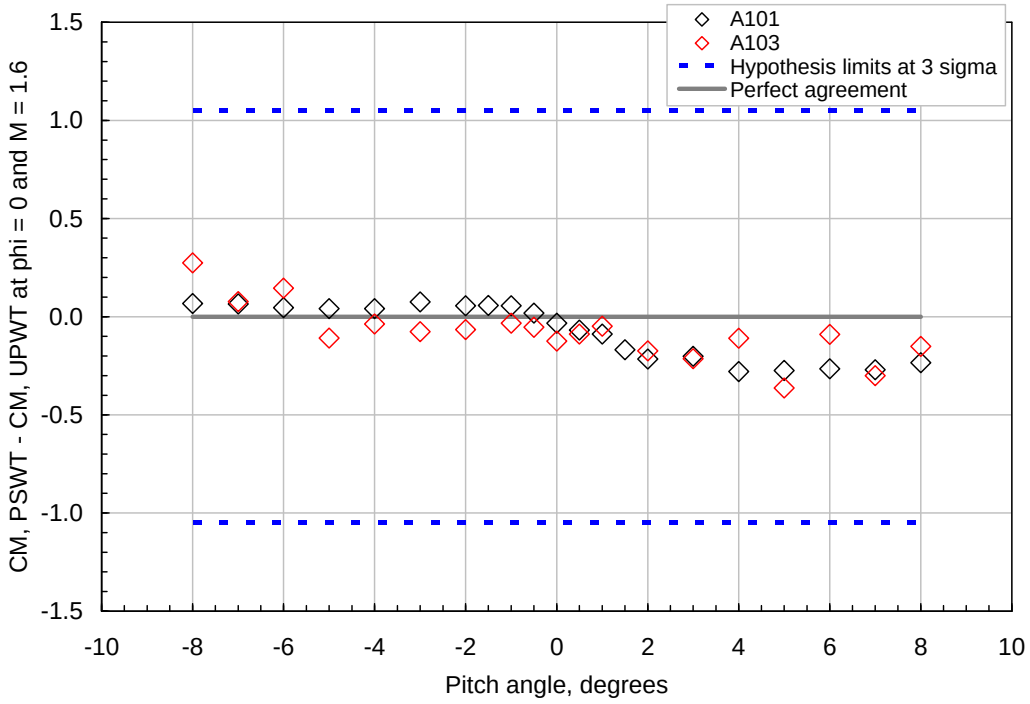

(a) Pitch runs at $\varphi = 0$.

Figure 13. CM PSWT-to-UPWT Comparison with Hypothesis Test.

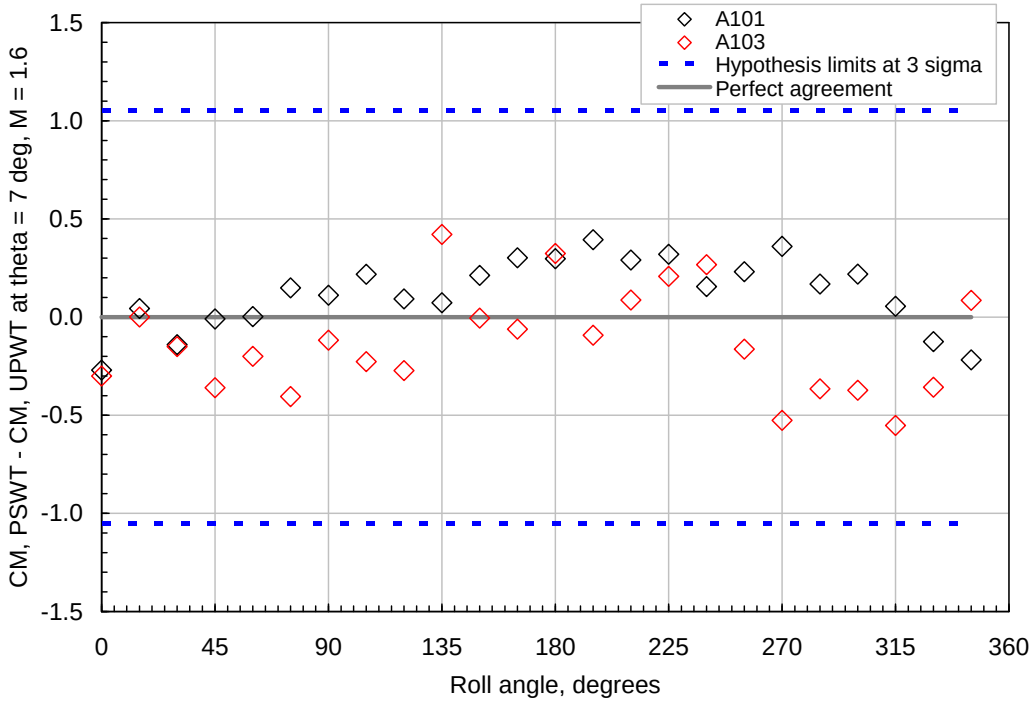

(b) Roll runs at $\theta = 7^{\circ}$.

Figure 13. Concluded.

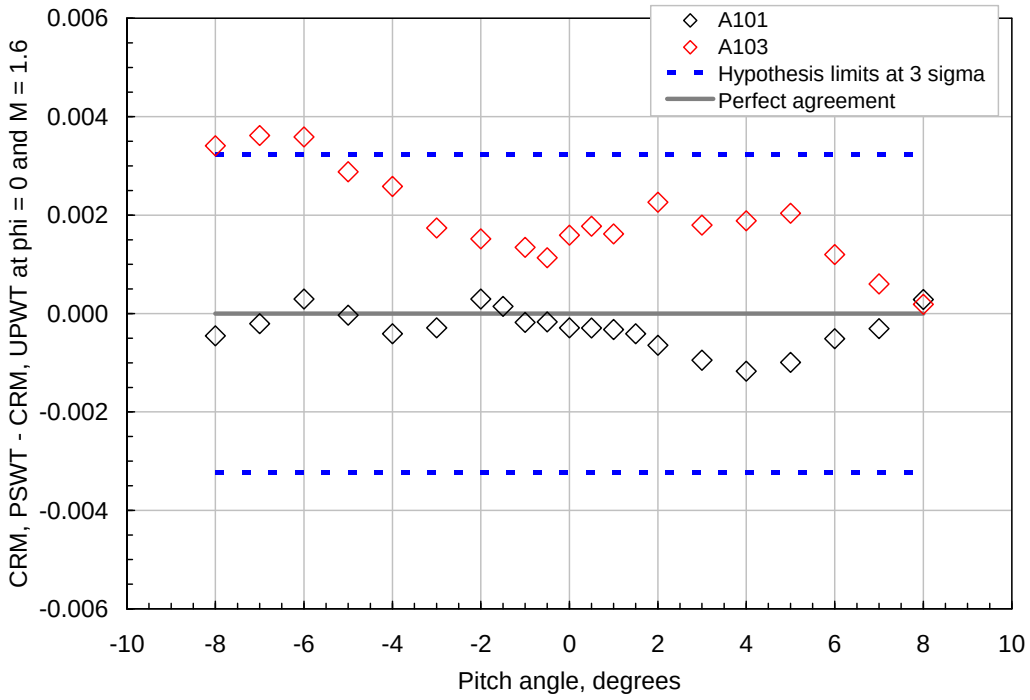

(a) Pitch runs at $\varphi = 0$.

Figure 14. CRM PSWT-to-UPWT Comparison with Hypothesis Test.

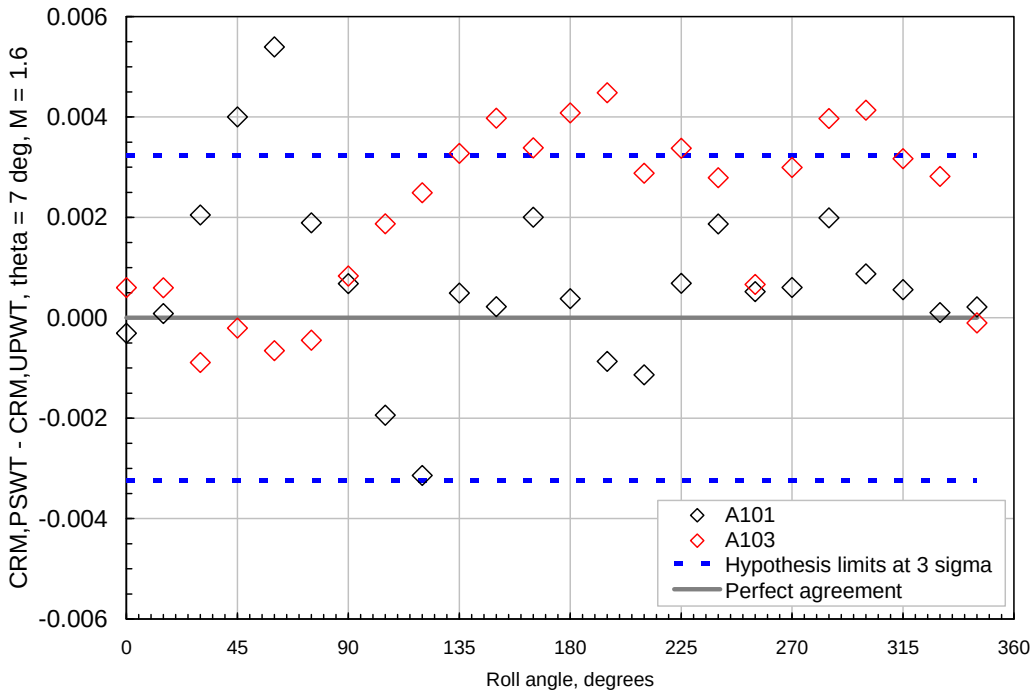

(b) Roll runs at $\theta = 7^{\circ}$.

Figure 14. Concluded.